LASER-EXCITED ACOUSTICS FOR CONTACT-FREE INSPECTION OF AEROSPACE COMPOSITES
АКУСТИКА З ЛАЗЕРНИМ ЗБУДЖУВАННЯМ ДЛЯ БЕЗКОНТАКТНОГО КОНТРОЛЮ АЕРОКОСМІЧНИХ КОМПОЗИТІВ

by Matthias Brauns, Fabian Lücking, Balthasar Fischer, Clint Thomson, and Igor Ivakhnenko

Ultrasonic testing (UT) is widely used for the nondestructive testing (NDT) of composite materials in the aerospace industry. Liquid- coupled piezoelectric ultrasonic transducers are the most common technology used in this field; however, liquid coupling agents are not always practical, economical, or compatible with materials that cannot get wet. Alternative couplant-free technologies such as air-coupled ultrasound or laser ultrasound (LUS) are available, but either lack the required sensitivity and resolution, or are very costly, large, and sensitive to surface condition and properties. In this paper, we introduce a new couplant-free approach using laser excitation and a commercially available optical microphone. This technique is termed laser-excited acoustics (LEA) NDT, which combines the advantages of a contact-free ultrasound technology with the potential for improved sensitivity and resolution required for NDT in industrial environments. We will demonstrate the capabilities of LEA on aerospace composite parts made of carbon and glass fiber–reinforced polymer (CFRP/GFRP) under realistic conditions.

Ультразвуковий контроль (UT) широко використовується для неруйнівного контролю (NDT) композитних матеріалів в аерокосмічній промисловості. П'єзоелектричні ультразвукові перетворювачі з рідинним зв'язком є наибільш розповсюдженою технологією, що використовується в цій області. Проте рідкі зв'язуючі не завжди практичні, економічні або сумісні з матеріалами, яким не можна намокати. Доступні альтернативні технології без зв'язуючої речовини, такі, як ультразвуковий контроль з повітряним зв'язком або лазерний ультразвук (LUS), але вони або не мають необхідну чутливість і роздільну здатність, або є дуже дорогими, завеликими та чутливими до стану та властивостей поверхні. В цій статті ми надаємо новий підхід без зв'язуючої речовини з використанням лазерного збуджування та оптичного мікрофона, що є у продажу. Цей метод називають неруйнівним контролем з використанням акустики з лазерним збудженням (LEA), який поєднує в собі переваги безконтактної ультразвукової технології з можливістю підвищення чутливості та роздільної здатності, що необхідні для неруйнівного контролю в промислових умовах. Ми продемонстрували можливості LEA на аерокосмічних композитних деталях з вуглецевого та армованого скловолокном полімеру (CFRP/GFRP) в реальних умовах.

Before we discuss the working principle of LEA, we will briefly review the basis of conventional ultrasonic NDT. In general, a pulser or emitter generates an ultrasound wave that travels through the sample and interacts with the features and interfaces of the material. After passing through the material, a receiver detects the transmitted or reflected ultrasound waves. The differences in the various techniques lie in how the ultrasound is generated and detected and in the arrangement of the sender and receiver.

Ultrasonic Testing with Piezoelectric Transducers. In conventional liquid-coupled ultrasound, piezoelectric transducers are widely used as emitters and receivers with a liquid coupling agent, such as water, between the transducer and the sample as shown in Figure 1b. The liquid facilitates the transfer of the ultrasonic wave energy. In cases where liquid cannot be used, the alternative has traditionally been air-coupled ultrasound. However, due to the large acoustic impedance mismatch between solids and air, even a small air gap between the transducers and sample strongly attenuates the transferred wave at each solid-to-air interface, and only a very weak signal arrives at the receiver, as shown in Figure 1a. This significantly limits the sensitivity of air-coupled ultrasound (Gaal et al. 2019). In some cases, the deleterious effects of poor impedance matching with air-coupled ultrasound can be lessened by resonant transducer designs, but these transducers are often very narrowband. In addition to impedance mismatch issues, the use of air-coupled ultrasound transducers for single-sided pulse-echo measurements is severely limited due to poor temporal performance and resonant ringing. This creates a front-wall "blind zone" where discontinuities close to the surface cannot be detected. Therefore, liquid-coupled ultrasound is preferred in the vast majority of industrial applications, even though this can introduce additional costs to automated scanning systems in the form of water squirters and immersion baths, and can present additional challenges regarding the testing of materials that are sensitive to liquids such as water (Vanderheiden et al. 2018). In order to achieve the same sensitivity with a contact-free ultrasonic NDT technology, it is crucial to reduce the number of solid-air interfaces for the ultrasound wave between the emitter, sample, and receiver.

In practical applications, measurement sensitivity for both liquid-coupled and air-coupled ultrasound is not the only performance-limiting factor. For automated robotic scanning systems, data quality also strongly depends on robustness against mis-

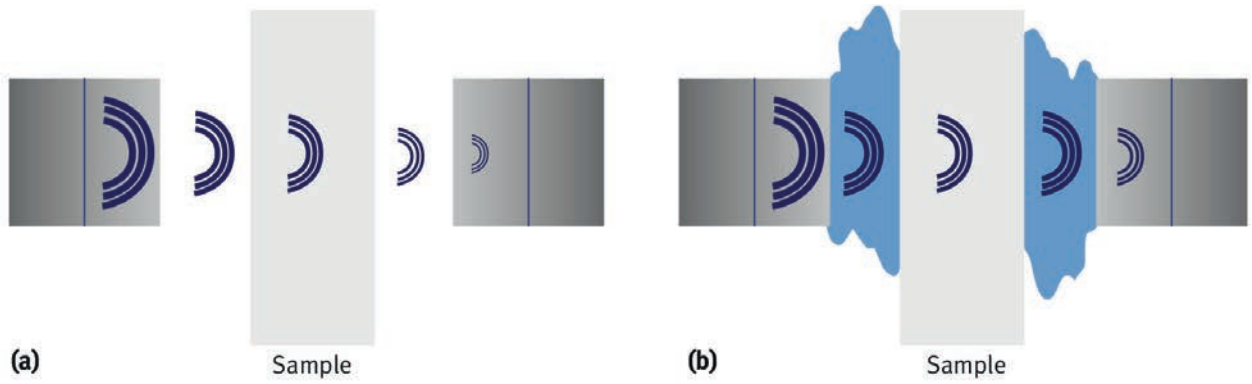

Figure 1. Schematic depiction of the attenuation of the ultrasound wave on its way from the emitter to the receiver: (a) air-coupled UT; (b) liquid-coupled UT.

Рис 1. Схематичне зображення загасання ультразвукової хвилі на шляху від випромінювача до приймача: (а) УЗК (UT) з повітряним зв'язком; (b) УЗК (UT) з рідинним зв'язком

alignments (angle and standoff) between sensor and sample. Both air- and liquid-coupled ultrasound are sensitive to angular misalignment with respect to the surface, leading to signal degradation even for misalignments of only a few degrees. While this is less relevant for simple flat sample geometries, sensitivity to misalignment becomes increasingly relevant for the ever-growing share of composite parts possessing large complex geometries of varying thickness that exhibit part-to-part variations. Here, significant costs can accrue in the form of precision robotics and tooling as well as sophisticated laser surface mapping and motion-control software.

Laser Ultrasound as a Contact-Free Alternative Some problems associated with air-coupled ultra-sound, such as impedance mismatch and temporal ringing, can be solved by LUS (Scruby and Drain 1990). Here, the ultrasound is both excited and detected by a laser. The excitation laser emits a short laser pulse onto the surface of the sample, where it is absorbed. The material locally heats up and expands on a timescale far below that of the thermal conductivity rate, which sends a broadband ultrasonic wave through the material. The ultrasound is generated directly inside the sample near the surface, which eliminates two of the four solid-air interfaces that would otherwise attenuate the signal. The laser-generated ultrasound waveform is very different from those emitted by piezoelectric transducers: since the laser pulse is very short (on the order of 10 ns), the excited ultrasound consists of a single, impulse-like peak. Historically, commercially available LUS systems have used powerful and expensive carbon dioxide lasers with complex laser-beam optical delivery systems to the scanning head. This makes them very difficult and costly to integrate into robotic scanning systems because optical fiber coupling is not possible at the operating wavelength of around 10 µm (Cuevas Aguado et al. 2015). More recently, experimental work has shown that laser excitation is also possible with solid-state fiber-coupled lasers at visible and near-infrared operating wavelengths (532 to 1064 nm), which allow for much smaller probe heads (Vandenrijt et al. 2018).

In traditional LUS, a second laser beam is directed at the sample surface for ultrasound detection. Part of the laser light is reflected back from the surface into the detector head, where the signal (the surface vibration of the sample due to the ultrasound wave) is measured by means of interferometry. This often re-

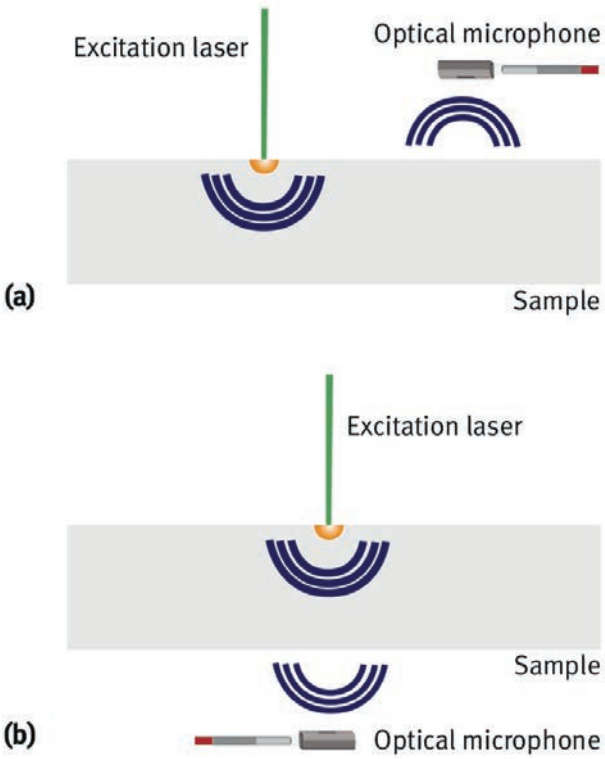

Figure 2. Laser-excited acoustics (LEA) setup with excitation laser and optical microphone: (a) on the same side of the sample (single-sided pitch-catch); (b) on opposite sides of the sample (through-transmission).

Рис. 2. Акустична установка з лазерним збуджуванням (LEA) зі збуджуючим лазером і оптичним мікрофоном: (а) на одній і тій же стороні зразка (одностороннє випромінювання-приймання); (b) на протилежних сторонах зразка (наскрізне пропускання)

quires complex optics as well as high-intensity laser light illuminating the surface to achieve an acceptable signal-to-noise ratio (SNR). Measuring the ultrasound directly on the sample surface enables a very large bandwidth up to 100 MHz. However, LUS can be sensitive to surface materials and condition (such as coatings, roughness, and reflectivity) and sometimes to standoff distance. Together with the high costs, these features have prevented the wider use of LUS in industry as a contact-free alternative to traditional ultrasonics over the past 40 years.

In summary, air-coupled ultrasound is limited in sensitivity and frequency bandwidth, and exhibits a blind zone for single-sided pulse-echo measurements. Liquid-coupled ultrasound needs an immersion fluid, which can add cost, and is not compatible with all materials. Finally, conventional LUS is a contact-free alternative with large bandwidth and high sensitivity, but presents high costs, is sensitive to surface conditions, and requires complex optics, making it impractical for most industrial applications.

Laser-Excited Acoustics: The Best of Both Worlds.

Here, we introduce our novel LEA technology approach, which solves many of the issues associated with the conventional techniques discussed in the previous section. In LEA, the setup is as follows: an excitation laser serves as the pulser and generates the ultrasound signal, while an optical microphone acts as the receiver (Fischer 2016; Fischer et al. 2019). LEA can operate in both standard arrangements for ultrasonic NDT: through-transmission testing with excitation laser and optical microphone on opposite sides of the sample and single-sided testing, where both sender and receiver are on the same side of the sample in a pitch-catch configuration, as illustrated in Figures 2a and 2b.

In contrast to most commercial systems available for conventional LUS, in LEA the visible or near-infrared excitation laser is fiber coupled, which enables a very compact sensor-head design for both single-sided pitch-catch and through-transmission setups.

Upon laser excitation, the ultrasound wave travels through the material, where it scatters off of the structural features. The ultrasound then propagates from the sample into the air, where the optical microphone (Figure 3a) detects the signal.

The detection principle of the optical microphone, as shown in Figure 3b, is based on laser interferometry. Inside the sensor head, measuring only a few millimeters, there is a small air cavity formed by two semitransparent mirrors. From a glass fiber, a laser beam couples through one of the mirrors into the cavity, where it is reflected back and forth. The length of the cavity can host a multiple of the laser's wavelength, so that the laser light constructively interferes. The light partly couples back into the glass fiber, and a photodetector converts its brightness into a voltage signal that is easily measurable. Sound and ultrasound alter the refractive index of the air, which affects the laser's wavelength in the cavity. This in turn changes the amount of light coupling back into the fiber, so that the photodiode detects a change in brightness. The output voltage of the photodiode therefore linearly changes over a wide range of acoustic pressures and over a frequency range extending from 10 Hz all the way up to 2 MHz. Over this large bandwidth, the frequency response is flat due to the detection principle, which does not involve any mechanical movement. In many instances, this reduces the effective blind zone associated with piezoelectric transducers.

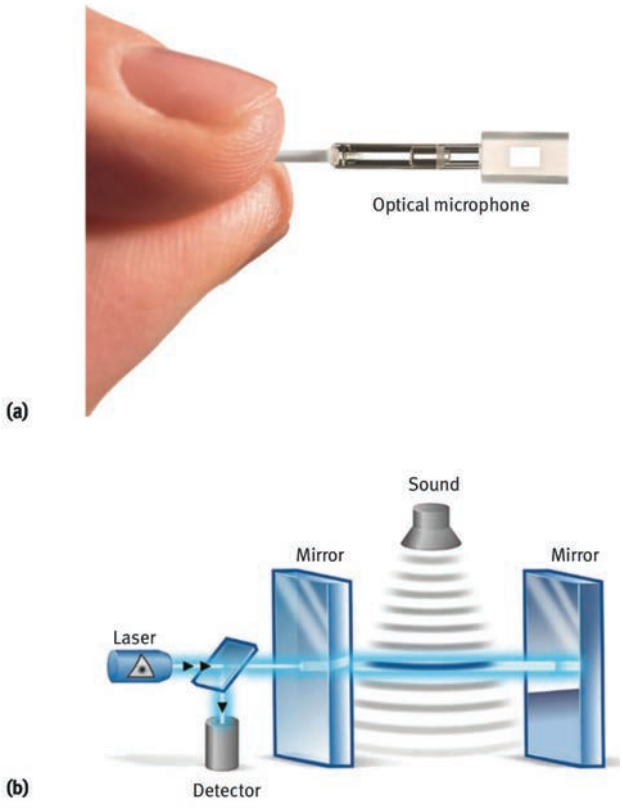

Figure 3. The optical microphone: (a) compact sensor head; (b) working principle.

Рис. 3. Оптичний мікрофон: (а) компактна сенсорна головка; (b) принцип роботи

Within the sensor head, the ultrasound pressure is measured directly in the air using laser detection; the ultrasound does not need to couple into a solid like it does for a piezoelectric receiver. From the four solid-air interfaces shown for air-coupled ultrasound in Figure 1a, only one interface (from the sample to air) remains. This greatly enhances the SNR associated with the measurement setup. At the same time, the ultrasound detection process is not affected by the optical quality of the sample surface (such as roughness), which enables its application for a wide

range of materials and geometries where previously contact-free LUS techniques could not be employed. Furthermore, both the excitation laser and the optical microphone are still operational even with an off-normal misalignment of ±5°. These features, combined with the compactness of the all-fiber-coupled probe head (measuring approximately 35 × 17 × 50 mm³), make LEA a viable contact-free alternative for NDT of parts with complex geometries and composition.

LEA of Sandwich Structures: Experimental Setup.

To assess the capabilities of LEA, measurements were performed on two honeycomb-core sandwich panels that are representative of structural materials widely used in aerospace applications. These panels consisted of a GFRP skinned panel and a CFRP skinned panel shown in Figures 4a and 4b. Both panels measured approximately 620 mm long × 230 mm wide × 13 mm thick and include various reference defects manufactured from polytetrafluoroethylene (PTFE) tape, graphite sheet, polyethylene backing material ("poly"), 1.3 mm deep core trenches, and release agent treated areas of various sizes (see the defect map in Figure 4c). While these reference defects were artificially placed in the sample structure, they realistically mimic various disbonds and foreign object debris that can occur at different stages of the composite production process. The standard NDT method used in industry for such parts is water- coupled through-transmission UT operating at a frequency of 0.5 to 1 MHz.

The experimental setup shown in Figure 5 was used to perform contact-free, through-transmission LEA ultrasound measurements on the samples. The excitation laser and the optical microphone were

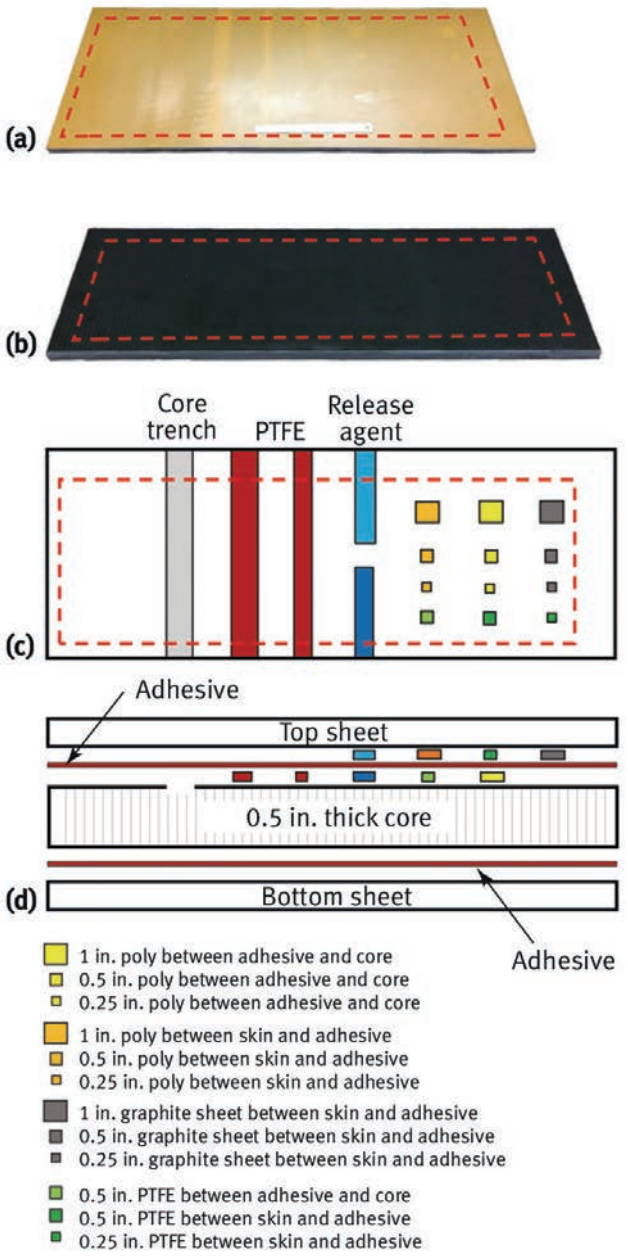

Figure 4. The experimental samples: (a) GFRP; (b) CFRP; (c) top-view map of reference defects; (d) side-view map of reference defects. The scanned area on each sample is marked by red dashed lines.
Рис. 4. Експериментальні зразки: (a) склопластик; (b) вуглепластик; (c) мапа еталонних дефектів, вид зверху; (d) мапа еталонних дефектів, вид збоку. Відскановану область на кожному зразку позначено червоними пунктирними лініями

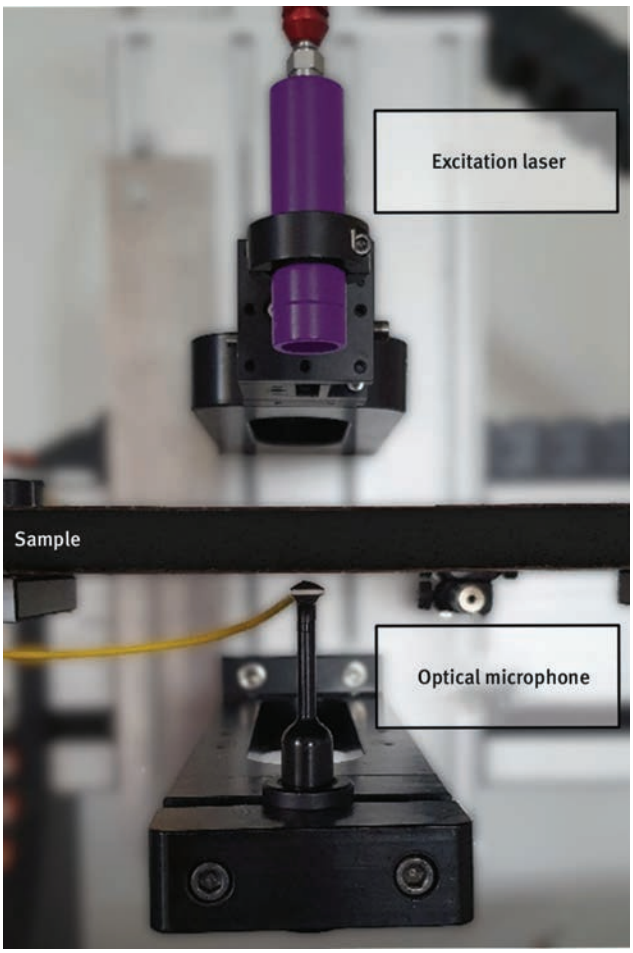

Figure 5. Measurement setup for the through-transmission measurements. The fiber-coupled excitation laser (purple) and the optical microphone were mounted on an X-Y scanning table. The sample stays in a fixed position between the laser and microphone.
Рис. 5. Вимірювальна установка для вимірювань при наскрізному пропусканні. Лазер збуджування з волоконним зв'язком і оптичний мікрофон було встановлено на сканувальному столі по X-Y. Зразок залишається в фіксованому положенні між лазером і мікрофоном

mounted to the probe fixture of an automated X-Y scanning table. With the sample fixed in position, we scanned the probe head across the sample area indicated by the red dashed lines in Figure 4. We set the step size to 0.5 mm in both the X- and Y-direction, far below the size of any defined defect and smaller than the honeycomb pitch of 3 mm. This ensured the scan resolution was limited by the resolution of the LEA setup itself, not by the scanning step size.

However, the scan step size can be deliberately set to other values such as 1 mm or 2 mm. For the laser excitation, we used a fiber-coupled pulsed laser with a wavelength of 532 nm. Every laser pulse corresponded to one measurement point on the sample with no waveform signal averaging. Hence, the pulse repetition rate, together with the step size, defined the scan speed. Different fiber-coupled excitation laser configurations were tested, with pulse repetition rates between 20 and 10 000 Hz. Using a 10 kHz laser setup, robotic scanning speeds of 1 to 2 m/s are achievable, on par with state-of-the-art liquid-coupled ultrasound scanner setups, and faster by approximately a factor of 10 when compared to air-coupled ultrasound setups. Furthermore, the optical microphone was tested in an eight-channel array configuration with a 2 mm pitch. In the array setup, the excitation laser beam profile is shaped to a line profile using a cylindrical lens, so that one laser excitation shot delivers eight autonomous detector signals simultaneously (see Figure 6). This allows for an additional eightfold increase in scan speed.

For the single-element receiver setup, the software controlling the scanner triggered the excitation laser pulse, and the ultrasound pressure amplitude was recorded using a sampling rate of 25 MHz. The resulting A-scan was saved for each measurement point. After the measurement, we determined the waveform peak maximum for each A-scan over a gated time window synchronized with the arrival of the initial signal. This maximum amplitude is plotted in the C-scans shown in Figures 7a and 7b, a 2D ultrasonic picture of the sample.

Results and Discussion

The C-scans of both samples reveal a number of different subsurface features not visible to the naked eye on the optically smooth sample. We observed well-defined areas of different sizes with a significantly attenuated signal amplitude, which we identified as the reference defects. While most defects were easily distinguishable, this was not true for the release agent and poly defects (blue, orange, and yellow in the Figure 4 defect map) in both samples. Interestingly, the only such defect visible at all was the smallest poly defect (marked by the white arrow in Figure 7a). The position of the invisible defects correlates with the large oval region of decreased signal amplitude extending over the right half of each sample, which is not referenced in the defect map. Here, the top sheets were unintentionally unbonded from the honeycomb core, perhaps due to the accidental spread of the release agent. Since these large unbonded areas coincided with the defect position between

Figure 6. Eight-channel array detector head. If combined with an excitation laser with a line-shaped beam profile, it increases the scanning speed by a factor of 8.

Рис. 6. Восьмиканальна матрична детекторна головка. В поєднанні зі збуджувальним лазером з лінійним профилем променя, він збільшує швидкість сканування у 8 разів

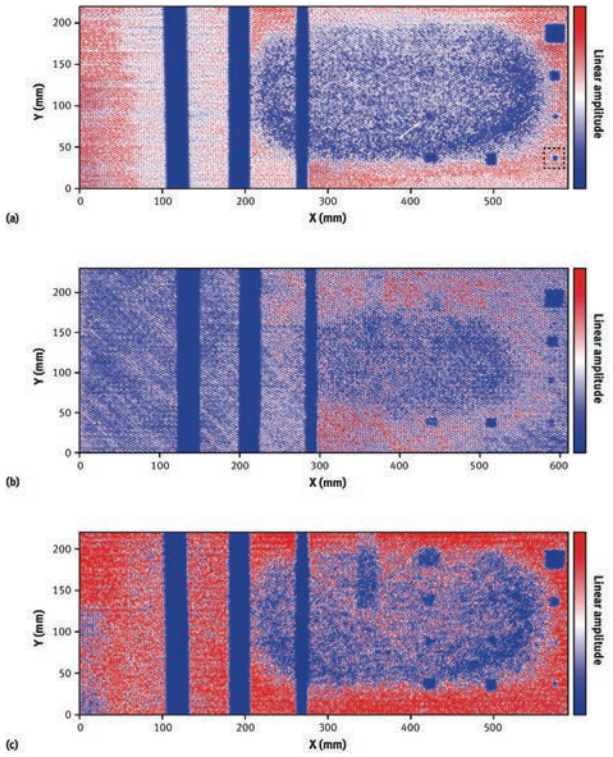

Figure 7. Ultrasonic C-scan images: (a) the GFRP sample shown in Figure 4a; (b) the CFRP sample shown in Figure 4b; (c) the same GFRP measurement data as in Figure 7a, but with a 1150 to 1200 kHz bandpass filter applied to each A-scan.

Рис. 7. Ультразвукові зображення від С-скану: (а) зразок склопластику, зображений на рис. 4а; (b) зразок вуглепластику, зображений на рис. 4b; (c) ті ж дані вимірювань в склопластику, що і на рис. 7а, але зі смуговим фільтром від 1150 до 1200 кГц, застосованим до кожного А-скану

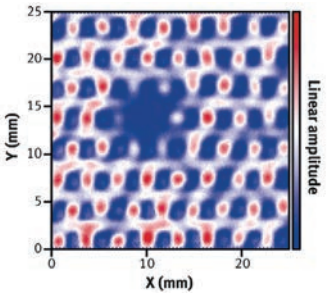

Figure 8. An enlargement of the area around the smallest reference defect shown in Figure 7a. The regular hexagonal pattern shows the internal honeycomb structure of the sample. The larger dark blue area is caused by the 6 mm inlay that was placed there as a reference defect.

Рис. 8. Збільшення області навколо найменшого еталонного дефекту, зображеного на рис. 7а. Правильний шестикутний визерунок вказує на внутрішню стільникову структуру зразка. Велика темна область з'явилась з-за 6-мм вкладишу, який помістили туди в якості еталонного дефекту

the top sheet and core, they masked the underlying defects in the C-scans.

For Figures 7a and 7b, a standard unfiltered data analysis was performed. However, since we have the whole frequency range from 50 kHz up to 2 MHz at our disposal, we can also analyze the data with more advanced frequency postprocessing methods, which are not possible with narrowband, air-coupled transducers. After applying a 1.15 to 1.20 MHz bandpass filter to every A-scan in Figure 7a for the GFRP panel, we again determined the peak amplitude at each position and plotted the results in the C-scan shown in Figure 7c. After applying the bandpass filter, we recognized the same reference defects that are visible in Figure 7a, but additionally, the release agent and poly defects, not apparent in Figure 7a, became visible as well. This demonstrates a strong advantage of the large bandwidth of LEA in comparison to piezoelectric-based ultrasound. Even though these defects are strongly obscured by another sample feature (the large disbond), the reference defects become visible by simple postprocessing of the existing data without the need for time-consuming and costly additional measurements at different transducer frequencies.

In order to demonstrate the measurement resolution of LEA, we zoomed in on one of the smallest defects present in the sample, a 0.25 × 0.25 in. (6.35 × 6.35 mm) PTFE insert between the GFRP top sheet and the adhesive film, as indicated by the dashed-line square in Figure 7a. Here, we performed a high-resolution scan with a step size of 0.2 mm, which is depicted in Figure 8. In addition to the clearly visible defect, we also observed the honeycomb structure as a very regular hexagonal pattern.

Again, we applied a bandpass filter to the data used in Figure 8 as shown in the C-scans in Figure 9. This allowed us to selectively investigate different aspects of the sample structure as well as different ultrasonic wave propagation modes through the sample structure.

Although ultrasonic modeling is required to fully explain the C-scan data shown in Figure 9, we speculate the following. For frequencies between 200 and 250 kHz, the transmitted signal was dominated by guided wave modes propagating through the honeycomb cell walls (Figure 9a). The signal amplitude and C-scan color scheme inverts for frequencies between 400 and 450 kHz, where the ultrasound passed almost exclusively through the air columns in the holes of the honeycomb structure (Figure 9b).

In Figure 9c, a bandpass filter between 750 and 800 kHz was applied. Here, both the honeycomb walls and the air columns exhibited high signal transmission, which leads to a more uniform C-scan with low contrast between the honeycomb wall and air columns. The only region with a significantly lower signal amplitude is the PTFE reference defect. This filtering scheme provides a clearer contrast between the defect and the rest of the honeycomb structure.

On the other hand, for the unfiltered data plotted in Figure 9d, there is less contrast between the defect and the cavities of the honeycomb structure; both exhibited the same dampened signal amplitude.

These examples demonstrate that the postprocessing of the LEA broadband data provides enhanced opportunities to selectively inspect the honeycomb walls, cell cavities, and any structural discontinuities. With conventional liquid-coupled or air-coupled ultrasound, this type of expanded analysis would not be possible without performing multiple measurements at different frequencies.

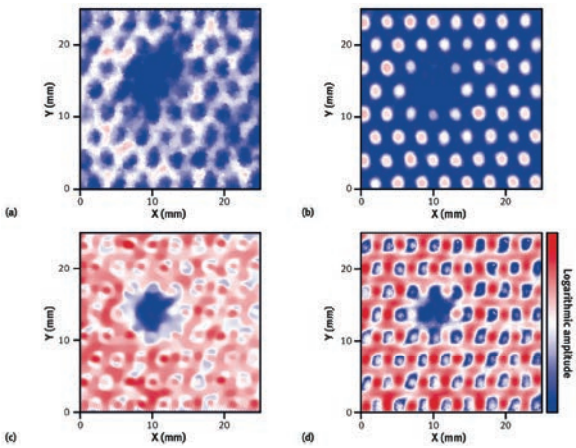

Figure 9. The measurement data from Figure 8 with a bandpass frequency filter applied with cutoff frequencies of: (a) 200 to 250 kHz, where the walls of the honeycomb core contribute the most to the signal; (b) 400 to 450 kHz, where the air columns in the honeycomb structure are revealed; (c) 750 to 800 kHz, where both features contribute to the signal, making the honeycomb structure less visible and highlighting the defect instead; and (d) the unfiltered data with the same logarithmic color scale used in Figures 9a through 9c. The signal amplitudes in each plot are normalized for clarity.

Рис. 9. Дані вимірювань з рис. 8 зі смуговим частотним фільтром, застосованим з частотами зрізу: (а) від 200 до 250 кГц, де стінки стільникового сердечника вносять найбільший вклад в сигнал; (b) від 400 до 450 кГц, де видно повітряні стовпи в стільніковій структурі; (c) від 750 до 800 кГц, де обидва елементи дають внесок в сигнал, роблячи стільникову структуру менш помітною і замість цього виділяючи дефект; (d) нефільтровані дані з тією ж самою логарифмічною шкалою, яка використовується на рис. 9а-с. Амплітуди сигналів на кожному графіку нормалізовано для наочності

Conclusion

In conclusion, LEA is a novel ultrasonic inspection technology that combines the advantages of standard liquid-coupled UT and contact-free inspection techniques. This is demonstrated by measurements of the CFRP and GFRP honeycomb sandwich panels used in our experiments, where high-resolution data were obtained using LEA as a fast, noncontact ultrasound scanning technique. These results show advantages in both resolution and sensitivity compared to state-of-the-art liquid-coupled and air-coupled ultrasound on structures such as honeycomb core sandwich materials (Thomson et al. 2015). Furthermore, the broadband ultrasound emission and detection achieved by the laser excitation and optical microphone setup allows for expanded frequency postprocessing, enabling the operator to inspect different aspects of the sample from a single measurement data set. This improves inspection reliability by increasing the likelihood for finding discontinuities that would otherwise be obscured using more narrowband piezoelectric-based ultrasonic technology. Apart from the technological advantage of an improved inspection, LEA also reduces overhead costs by rendering water management and disposal unnecessary.

The combination of these properties makes LEA a compact and affordable couplant-free alternative to traditional liquid-coupled and air-coupled ultrasound for NDT of a variety of aerospace composite materials.

AUTHORS

Matthias Brauns: XARION Laser Acoustics GmbH, Ghegastraße 3, 1030 Vienna, Austria; m.brauns@xarion.com

Fabian Lücking: XARION Laser Acoustics GmbH, Ghegastraße 3, 1030 Vienna, Austria

Balthasar Fischer: XARION Laser Acoustics GmbH, Ghegastraße 3, 1030 Vienna, Austria

Clint Thomson: Northrop Grumman Corp., Aeronautics Systems Sector, Aerospace Structures Business Unit, Inspection Development Group, UT02-YC14, PO Box 160433, Clearfield, Utah, 84016-0433, USA

Igor Ivakhnenko: Northrop Grumman Corp., Aeronautics Systems Sector, Aerospace Structures Business Unit, Inspection Development Group, UT02-YC14, PO Box 160433, Clearfield, Utah, 84016-0433, USA

REFERENCES

1. Cuevas Aguado, E., C. Galleguillos, C. García Ramos, and F. Lasagni, 2015, "Laser Ultrasonics Inspections of Aeronautical Components Validated by Computed Tomography," *7th International Symposium on NDT in Aerospace*, 16–18 November, Bremen, Germany.
2. Fischer, B., 2016, "Optical Microphone Hears Ultrasound," Nature Photonics, Vol. 10, pp. 356–358, https://doi.org/10.1038/nphoton.2016.95.
3. Fischer, B., F. Sarasini, J. Tirillo, F. Touchard, L. Chocinski-Arnault, D. Mellier, N. Panzer, R. Sommerhuber, P. Russo, I. Papa, V. Lopresto, and R. Ecault, 2019, "Impact Damage Assessment in Biocomposites by Micro-CT and Innovative Air-Coupled Detection of Laser-Generated Ultrasound," Composite Structures, Vol. 210, pp. 922–931, https://doi.org/10.1016/j.compstruct.2018.12.013.
4. Gaal, M., D. Kotschate, and K. Bente, 2019, "Advances in Air-Coupled Ultrasonic Transducers for Non-Destructive Testing," Proceedings of Meetings on Acoustics, Vol. 38, No. 1, https://doi.org/10.1121/2.0001072.
5. Scruby, C.B., and L.E. Drain, 1990, Laser Ultrasonics Techniques and Applications, CRC Press.
6. Thomson, C.D., I. Cox, M.T.A. Ghasr, K.P. Ying, and R. Zoughi, 2015, "Ultrasonic, Microwave, and Millimeter Wave Inspection Techniques for Adhesively Bonded Stacked Open Honeycomb Core Composites," AIP Conference Proceedings, Vol. 1650, https://doi.org/10.1063/1.4914738.
7. Vanderheiden, B., C. Thomson, I. Ivakhnenko, and C. Garner, 2018, "Transition to High Rate Aerospace NDI Processes," AIP Conference Proceedings, Vol. 1949, No. 1, https://doi.org/10.1063/1.5031500.
8. Vandenrijt, J.-F., F. Languy, C. Thizy, and M. Georges, 2018, "Laser Ultrasound Flexible System for Non-contact Inspection of Medium Size and Complex Shaped Composite Struc- tures Made of Carbon Fiber Reinforced Polymer," Proceedings of the 18th International Conference on Experimental Mechanics, Vol. 2, No. 8, https://doi.org/10.3390

Permission to Reprint, 04.10.2021:
The American Society for Nondestructive Testing, Inc.
CITATION
Materials Evaluation 79 (1): 28–37
https://doi.org/10.32548/2021.me-04188